Modeling and control of standalone hybrid (Wind / photovoltaic) generator

M. F. Almi, H. Belmili, B. Bendib, S.Boulouma

Unité de Développement des Equipements Solaires
(UDES) / EPST- Centre de Développement des
Energies Renouvelables
Bou Ismail, Algérie
fayalmi@hotmail.fr

M. Arrouf

Department of Electrical Engineering,
University of Batna
Batna, Algerie
karrouf@hotmail.fr

Abstract—**This paper describes the analysis and design of a hybrid (Wind/PV) power system for domestic applications in rural and remote areas, in this system each component is modeled with respect to its application type. The sizing of this system is mainly based on the price quality factor of the extracted energy. The system under study is modeled under the Matlab/Simulink simulation platform then it is tested for different meteorological conditions. In this design each system is controlled individually to operate in its maximum power point (MPPT). The simulation results and the sensibility analysis show that our generator is able to exploit the complementarily between the two energy sources (wind/ PV) and provides a reliable energy production.**

Keywords: wind; Pv; mppt; control; inverter.

I.   INTRODUCTION

Nature offers free, inextinguishable and widely available energy sources. The most common renewable energies are wind and photovoltaic energies. The rapid development in semiconductor technologies made these energies more profitable. These energy sources are usually used in standalone fashion or combined together in a hybrid framework, also, they can be isolated or grid connected. Given that the energy yield of these systems is highly dependent on meteorological conditions, the combination of many sources in a hybrid framework seems to be a reasonable solution to ensure stable energy production. In order to achieve a balance between to production and the consumption, energy storage elements are required. Moreover, complementary energy sources such as diesel generators are necessary in case of outages. A multi-source power supply must obey some connection architecture. Also, a convenient production monitoring of the sources with respect to loads allows fulfillment of electrical need as well as an optimal utilization of the produced energy. In this regard, this paper conducts a survey on the optimal architecture of a standalone network and the well suited monitoring and supervision strategy.

II.   HYBRID SYSTEM CONFIGURATION

A typical hybrid energy generation system is shown in Fig. 1; its main constituents are a 1Kw wind turbine generator (WTG), a 1Kw photovoltaic array. The energy storage system is a Battery bank that is initially charged to 50% of its maximum capacity which can be chosen according to the desired autonomy. The whole system supplies a AC load of 1Kw.
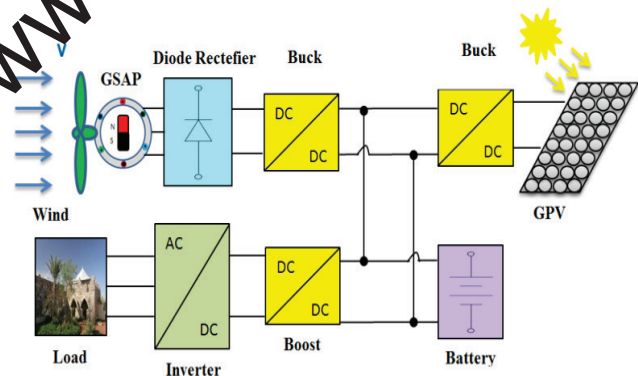

Figure 1.   The studied hybrid system configuration

III.   WIND MODELING

A. Wind Speed

Wind speed, regarding its statistical distribution is of paramount importance in every wind plant; hence it is a decisive factor in assessing energy production and its efficiency [1].

In this work, the wind speed is modeled as a deterministic, non-stationary signal given as the sum of sinusoids as follows:

$$V_v(t) = 10 + 0.2\sin(0.1047t) + 2\sin(0.2665t) + \\ + \sin(1.293t) + 0.2\sin(3.6645t) \tag{1}$$

B. Wind turbine

The mechanical power P_{wind} of the wind turbine is given by:

$$P_{wind} = \frac{1}{2}.\rho.S_t.C_p(\lambda,\beta).V^3 \qquad (2)$$

The computation of the power coefficient C_p requires the use of blade element theory and the knowledge of blade geometry. In this paper, the wind turbine used corresponds to the one with the numerical approximation developed in [2], where the power coefficient is given by:

$$C_p = 0.73\left(\frac{151}{\lambda_i} - 0.58\beta - 0.002\beta^{2\ 14} - 13.2\right)e^{-\frac{18\ 4}{\lambda_i}} \qquad (3)$$

$$\lambda_i = \frac{1}{\frac{1}{\lambda - 0.02\beta} - \frac{0.003}{\beta^3 + 1}} \qquad (4)$$

The power coefficient C_p is a function of the pitch angle β of rotor blades and of the tip speed ratio λ lambda, which is given by:

$$\lambda = \frac{\Omega \times R}{V_w} \qquad (5)$$

C. Permanent Magnet Synchronous Generator (PMSG)

Permanent magnet synchronous generators (PMSG's) are typically used in small wind turbines for several reasons including high efficiency, gearless, simple control...etc. [3].

A simple steady-state model, such as those used in other types of machines, has been chosen in order to evaluate the behavior of these types of machines, with the following assumptions:

- Saturation is neglected;
- Internal voltage or back emf is sinusoidal(harmonic components are neglected);
- Eddy currents and hysteresis losses are negligible $L_{sd}= L_{sq}$.

$$V_{sd} = -R_s I_{sd} - L_{sd}\frac{dI_{sd}}{dt} + \omega L_{sq}I_{sq} \qquad (6)$$

$$V_{sq} = -R_s I_{sq} - L_{sq}\frac{dI_{sq}}{dt} - \omega L_{sd}I_{sd} + \omega\psi_f \qquad (7)$$

$$T_{em} = \frac{3}{2}p(\psi_{sd}I_{sq} - \psi_{sq}I_{sd}) \qquad (8)$$

$$\psi_{sd} = L_{sd}I_{sd} + \psi_f \qquad (9)$$

$$\psi_{sq} = L_{sq}I_{sq} \qquad (10)$$

$$T_{em} = \psi_f I_{sq} + p(L_{sd} - L_{sq})I_{sd}I_{sq} \qquad (11)$$

$$T_{em} = \psi_f I_{sq} \qquad (12)$$

- Mechanical drive train :

$$T_{me} - T_{em} - f.\Omega = j\frac{d\Omega}{dt} \qquad (13)$$

T_{me} : Mechanic torque

T_{em} : Electromagnetic torque

$f.\Omega$: Friction torque

j : Moment of inertia.

f : Viscous Coefficient friction.

D. MPPT Control Strategy For Wind Turbine System

For small-scale wind generator system (say, the rated output power bellow 1kW), a synchronous generator is used [4].

According to the operation theory of wind turbine, the maximum output power of wind generator depends on the optimal tip speed ratio λ_{opt}. In terms of this, the MPPT is controlled to track the maximum power of wind turbine and the battery charging voltage in such a way:

$$P_{wind} = \frac{1}{2}.\rho.S_t.C_p(\lambda,\beta).V^3 \qquad (14)$$

$$C_{p\max} = C_p(\lambda_{\max})$$

$$P_{opt} = K_{opt}.\Omega_{ref}^3 \qquad (15)$$

$$K_{opt} = \frac{1}{2}.\rho.\pi.C_{p\max}.\frac{R^5}{\lambda^3} \qquad (16)$$

$$\Omega_{ref} = \frac{V.\lambda_{\max}}{R} \qquad (17)$$

Fig. 2 shows a family of the wind turbine generated power curves with respect to the speed Ω. The black colored plot shows the corresponding maximum power points
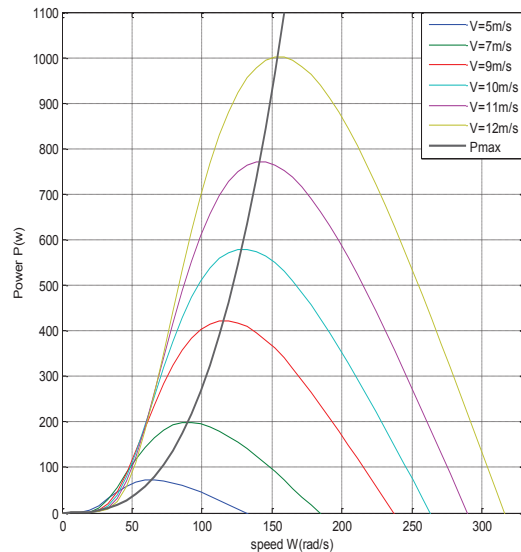

Figure 2.   Wind turbine power curves for various wind speeds

IV. PHOTOVOLTAIC GENERATOR MODEL

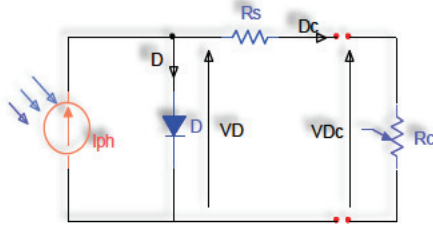The modeling of a photovoltaic cell can be carried out according to various levels of complexity.

Figure 3.   Simplified electrical model of photovoltaic cell

R_s: series resistance

R_c: load

I_D, V_D: diode current and voltage

I_{DC}, V_{DC}: The current voltage of a PV cell

The model translates a reference point (I_{ref}, V_{ref}) to a new point (I, V) according to the equations below [5, 6].

$$I_{ref} = I_{sc}\left[1 - C_1\left[\exp\left(\frac{V_{ref}}{C_2 . V_{co}}\right) - 1\right]\right] \quad (18)$$

$$C_1 = \left(1 - \frac{I_{mp}}{I_{sc}}\right)\exp\left(\frac{-V_{mp}}{C_2 V_{co}}\right) \quad (19)$$

$$C_2 = \frac{\left(\frac{V_{mp}}{V_{co}} - 1\right)}{Ln\left(1 - \frac{I_{mp}}{I_{sc}}\right)} \quad (20)$$

$$\Delta T = T - T_{ref} \quad (21)$$

$$\Delta I = \alpha\left(\frac{E}{E_{ref}}\right)\Delta T + \left(\frac{E}{E_{ref}} - 1\right)I_{sc} \quad (22)$$

$$= -\beta.\Delta T - R_s.\Delta I \quad (23)$$

$$V = V_{ref} + \Delta V \quad (24)$$

$$I = I_{ref} + \Delta I \quad (25)$$

α : Current variation coefficient according to temperature.

β : Voltage variation coefficient according to temperature.

A. Maximum power point tracking

We have chosen the incremental conductance algorithm (INC) for its good quality/price ratio and ease of implementation [7, 8].
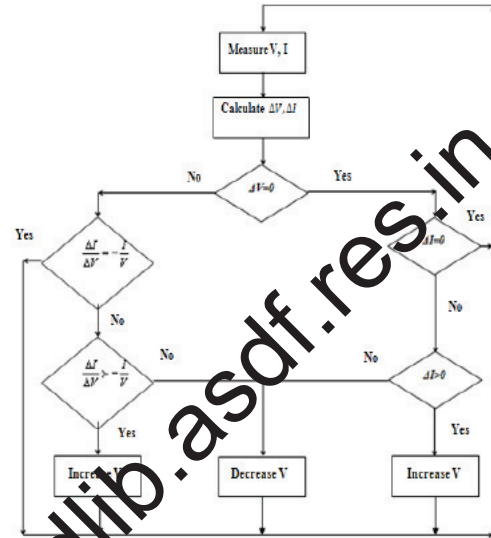

Figure 4.   Incremental conductance technique flowchart

V. MODELING OF THE BATTERY

For the battery bank modeling, Thevenin's equivalent circuit of the battery is used [9, 10]; the parallel combination of capacitance C_b and resistance R_b is used to describe the energy stored by the battery and R_{in} as internal resistance.

The equivalent capacitance C_b is given by,

$$C_b = \frac{(KWh \times 3600 \times 1000)}{0.5\left(V_{oc\,max}^2 - V_{oc\,min}^2\right)} \quad (26)$$

VI. MODELING OF POWER ELECTRONICS

A. Inverter modeling

The output voltage of the inverter, V_{op}, is the voltage between V_A and V_B, where V_A and V_B are the potentials at the points A and B with respect to the neutral potential $(V_N = 0)$. The voltage vector $[V_A V_B]^T$ can be expressed as:

$$\begin{bmatrix} V_A \\ V_B \end{bmatrix} = \frac{1}{2}V_{DC}\begin{bmatrix} 1 & -1 \\ -1 & 1 \end{bmatrix}\begin{bmatrix} a \\ b \end{bmatrix} \quad (27)$$

Where "a" and "b" are the switching signals for the four IGBTs with "1" representing the turn-on state and "0" representing the turn-off state, V_{DC} is the DC link voltage [11, 12].

The output voltage of the inverter can have three values:

$$V_o(1 \; 0) = V_{DC}; V_o(0 \; 1) = -V_{DC}$$

And

$$V_o(1 \; 1) = V_o(0 \; 0) = 0$$

B. *Three-phase diode bridge rectifier*

The diode rectifier is the most simple, cheap, and rugged topology used in power electronic applications. The drawback of this diode rectifier is its inability to work in a bi-directional power flow.

It is assumed that the AC power generated from the generator is converted into DC power through diode bridge rectifier circuits [13].

$$P = 3.V.I = V_{DC}.I_{DC} \tag{28}$$

$$V_{DC} = \frac{3}{\pi} \int_{-\frac{\pi}{6}}^{\frac{\pi}{6}} V_{LL\max}.\cos(\theta).d\theta \tag{29}$$

$$V_{DC} = \frac{3}{\pi} V_{LL\max} \tag{30}$$

$$V_{LL\max} = \sqrt{2}.V_{LL} \tag{31}$$

$$V_{DC} = \frac{3}{\pi} \sqrt{2}.V_{LL} \tag{32}$$

From this, the relationship between V_{DC} and phase voltage V is

$$V_{DC} = \frac{3}{\pi} \sqrt{6}.V \tag{33}$$

Then the relation between I_{DC} and *I* is

$$I_{DC} = \frac{\pi}{\sqrt{6}} I \tag{34}$$

C. *DC/DC Boost Converter*

In this model, the boost converter has been controlled to yield constant output DC voltage level, by varying the duty ratio, α in response to variations in V_i.

The relation between the input and output voltage and currents of the boost converter is expressed by the following equations [14].

$$V_o = \frac{1}{1-\alpha} V_i \tag{35}$$

$$I_o = (1-\alpha)I_i \tag{36}$$

D. *DC/DC Buck converter*

The average output voltage of the buck converter is given by

$$V_o = \alpha.V_i \tag{37}$$

The DC voltage at the converter output feeds the battery DC bus which is nearly constant. Assuming negligible converter losses, the average output current is of the buck converter is given by [15].

$$I_o = \frac{I_i}{\alpha} \tag{38}$$
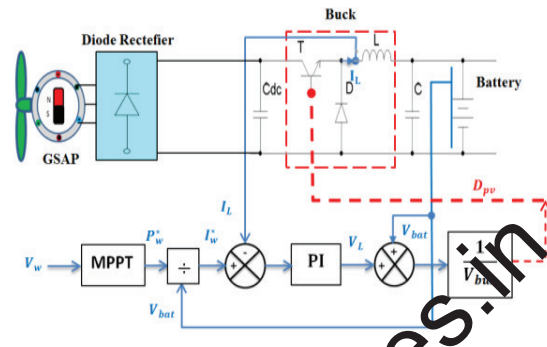
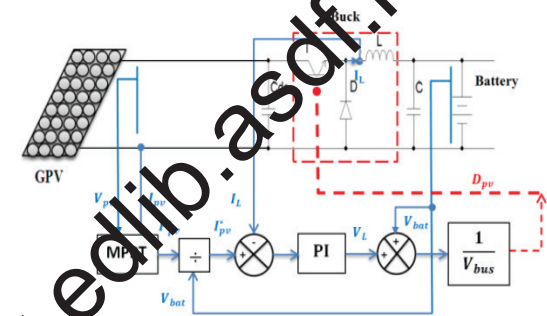## VII. PROPOSED CONTROL STRATEGY

Figure 5.   Wind control

Figure 6.   GPV control
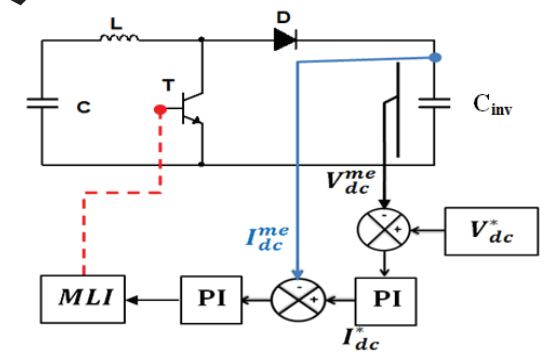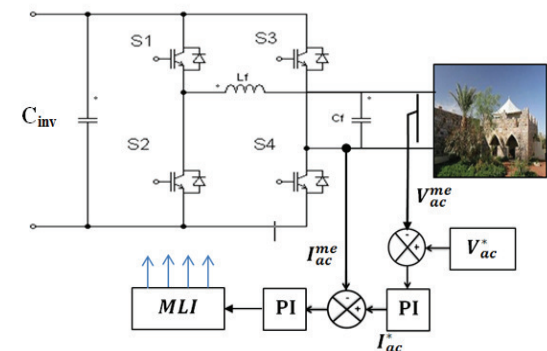

Figure 7.   DC/DC Boost control

Figure 8.   DC/AC Inverter control

VIII.   SIMULATION RESULTS

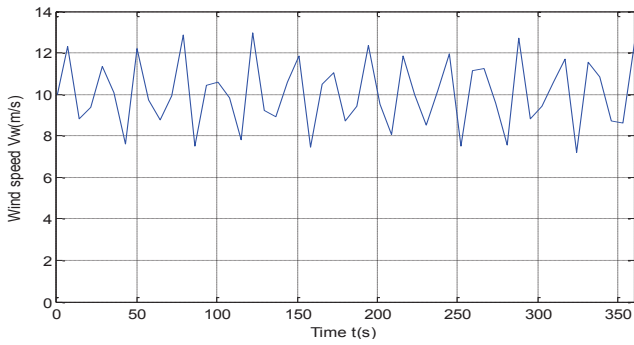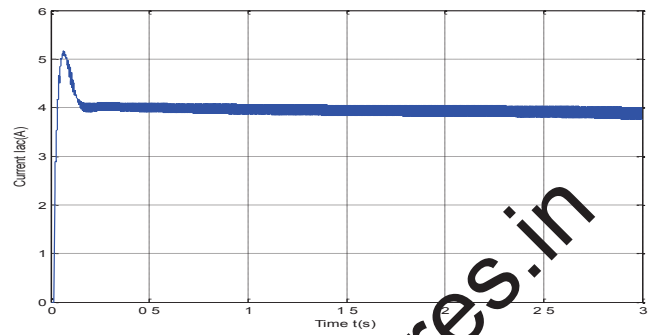Figure 9.   Wind speed

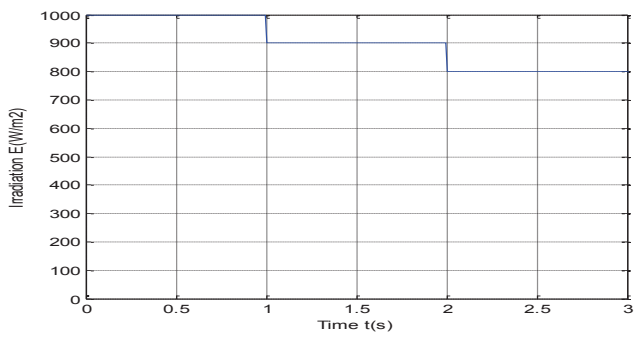Figure 13.   Rms current of PMSG

Figure 10. Solar irradiation
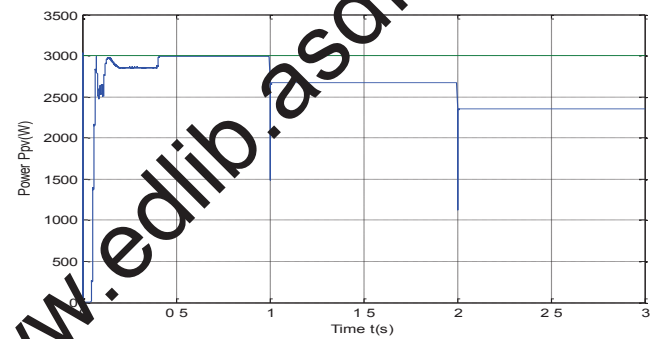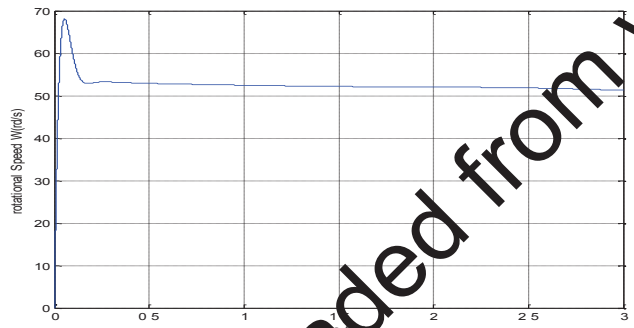

Figure 14. Power of GPV

Figure 11. Rotational speed of PMSG
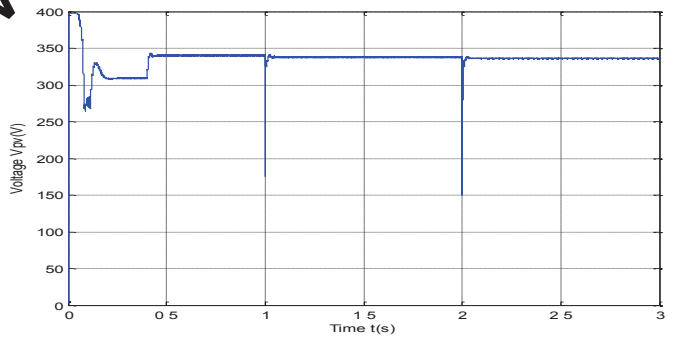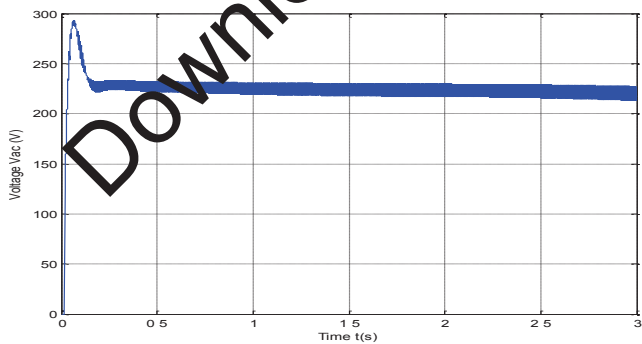

Figure 15. Voltage of GPV
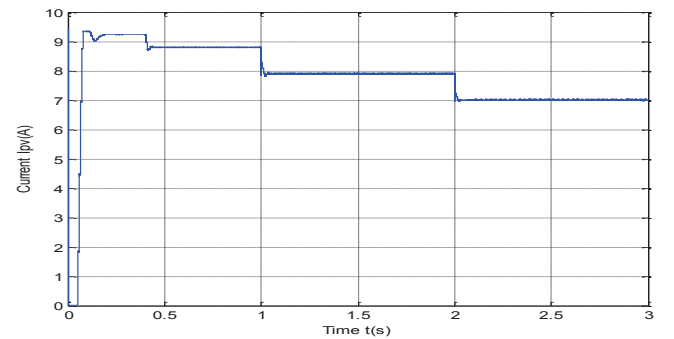

Figure 12. Rms voltage of PMSG
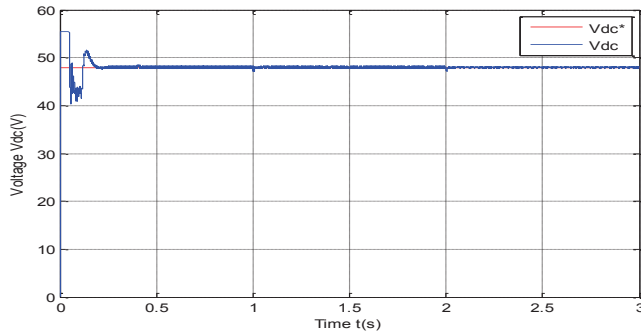
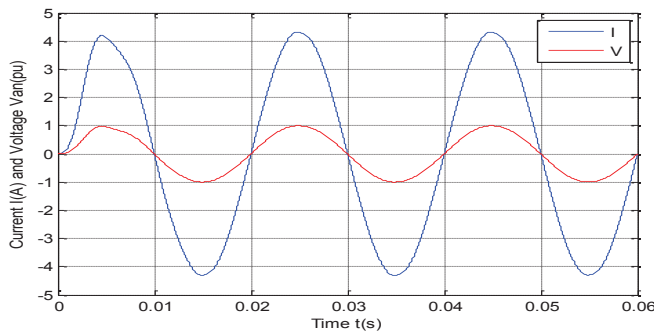

Figure 16. Current of GPV

Figure 17. Voltage of DC bus

Figure 18. Voltage and current of AC load

IX. CONCLUSION

In this paper, we have elaborated mathematical models for the components of a hybrid (Wind-PV) energy system. The variation of solar irradiance given in Fig. 12 and that of the wind speed given in Fig. 11 allow as assessing their influence upon the overall behavior of the system. In the light of the obtained simulation results, we conclude that the response of the voltage across the battery to changes in the wind speed is relatively fast despite the consequent influence of the solar irradiance on the photovoltaic generated power. Finally, we see that the energy produced by the system remains constant, according to the load with a voltage of 220V. This is due to the power stored in the batteries, which will be used to compensate energy lacks and the efficiency of the control strategy we have used.

REFERENCES

[1] A.Mirecki "Etude comparative de chaînes de conversion d'énergie dédiées à une éolienne de petite puissance" Thèse préparée au Laboratoire d'Electrotechnique et d'Electronique Industrielle de l'ENSEEIHT Unité Mixte de Recherche CNRS N 5828 N d'ordre : 2259 Année 2005

[2] R. Melício , V.M.F. Mendes , J.P.S. Catalão " Comparative study of power converter topologies and control strategies for the harmonic performance of variable-speed wind turbine generator systems " Energy 36 (2011) 520e529.

[3] F. Valenciaga and P. F. Puleston "Supervisor Control for a Stand-Alone Hybrid Generation System Using Wind and Photovoltaic Energy" ieee transactions on energy conversion, vol. 20, no. 2, june 2005.

[4] Z. Lubsony, Wind Turbine Operation in Electric Power Systems, Springer-Verlag, Germany, 2003.

[5] A. Hoque et K. A. Wahid « New mathematical model of a photovoltaic generator (PVG) » Journal of Electrical Engineering The Institute of Engineers, Bangladesh Vol. EE 28, No. 1, June 2000.

[6] Project group INTRO-712, "Residential Microgrid System", Aalborg University, 2008.

[7] D. Sera,R.Teodorescu,T.kerekes « Teaching Maximum Power Point Trackers Using a Photovoltaic Array Model with Graphical User Interface » Photovoltaic Specialists Conference, 2000. Conference Record of the 28th IEEE 15-22 Sept. 2000 Pages:1699 – 1702.

[8] Mukund R. Patel, Wind and Solar Power Systems. CRC Press, USA, 1999.

[9] S. Diaf, D. Diaf, M. Belhamel, M. Haddadi, A. Louche "A methodology for optimal sizing of autonomous hybrid PV/wind system" Energy Policy 35 (2007) 5708–5718.

[10] Tamer H. Abdelhamid and Khaled El-Naggar "Optimum estimation of single phase inverter's switching angles using genetic based algorithm," Alexandria Engineering Journal, Vol. 44, No.5, 751-759, 2005.

[11] J.Martinez, A.Medina "A state space model for the dynamic operation representation of small-scale wind-photovoltaic hybrid systems" Renewable Energy 35 (2010) –1168.

[12] N.A. Ahmed, A.K. Al-Othman, M.R. AlRashidi "Development of an efficient utility interactive combined wind/photovoltaic/fuel cell power system with MPPT and DC bus voltage regulation" Electric Power Systems Research 81 (2011) 1096–1106

[13] K.Y.Lo, Y.M.Chen, and Y.R.Chang "MPPT Battery Charger for Stand-Alone Wind Power System" IEEE TRANSACTIONS ON POWER ELECTRONICS, VOL. 26, NO. 6, JUNE 2011.

[14] M. G. Molina, D. H. Pontoriero, P. E. Mercado. "An efficient maximum-power-point-tracking controller for grid-connected photo-voltaic energy conversion system". Brazilian Journal of Power Electronics, vol.12, no.2, pp.147–154, 2007.

[15] L. Barote and C. Marinescu "Renewable Hybrid System with Battery Storage for Safe Loads Supply" Paper accepted for presentation at the 2011 IEEE Trondheim PowerTech.

[16] Y.C.Qin,N.Mohan,R.West,etR.Bonn "Status and needs of power electronics for photovoltaic inverters" Sandia National Laboratories 2002.

[17] J. S. Thongam, P. Bouchard, R. Beguenane, I. Fofana and M. Ouhrouche "Sensorless Control of PMSG in Variable Speed

[18] Wind Energy Conversion Systems" The International Power Electronics Conference 978-1-4244-5393-1/10/$26.00 ©2010 IEEE.

APPENDIX.

Shell 150-PC array Characteristics

$I_{sc} = 4.8A; I_{mp} = 4.4A; V_{so} = 43.4V; V_{mp} = 34V$

$R_s = 0.529\Omega; \alpha = 2mA/C^0; \beta = -152mV$

$N_s = 10; N_p = 2$

PMSG parameters [17] :

$P_n = 1.12KW; R_s = 8.39\Omega; L_s = 0.08483H$

$V = 230V; N = 500rpm; P = 3$

Turbine parameters [17] :

$P_n = 1.32KW; R = 1.26m; \lambda_{max} = 6.597; C_{p\max} = 0.48$

$j = 1.5Kg.m^2; \rho = 1.14Kg/m^3; V = 240V; V_{DC} = 400V$